CIRCUMFERENTIAL INLET DISTORTIONS IN AN AXIAL FLOW COMPRESSOR

FRANK R. CARTER

CIRCUMFERENTIAL INLET DISTORTIONS IN AN AXIAL FLOW COMPRESSOR

FRANK R. CARTER

MAY 1958

Department of Aeronautical Engineering
MASSACHUSETTS INSTITUTE OF TECHNOLOGY
Cambridge 39, Massachusetts

CIRCUMFERENTIAL INLET DISTORTIONS IN AN AXIAL FLOW COMPRESSOR

by

LT FRANK R. CARTER, U. S. NAVY

B. S., United States Naval Academy, 1950

B. S. A. E., United States Naval Postgraduate School, 1957

SUBMITTED IN PARTIAL FULFILLMENT OF THE
REQUIREMENTS FOR THE DEGREE OF
MASTER OF SCIENCE

at the

MASSACHUSETTS INSTITUTE OF TECHNOLOGY

1958

CIRCUMFERENTIAL INLET DISTORTIONS IN AN AXIAL FLOW COMPRESSOR

by

Frank R. Carter

Submitted to the Department of Aeronautical Engineering on May 26, 1958, in partial fulfillment of the requirements for the degree of Master of Science.

ABSTRACT

Due to the importance of inlet velocity profile distortions in axial compressors of high-speed, gas turbine driven aircraft, this study has been made to investigate velocity inlet defects and their attentuation for the case of an isolated rotor in an axial flow compressor. The effects of various profile generators at several flow rates were investigated, and the actual measured effect of the rotor on the inlet velocity distortion was compared with the theoretically predicted downstream profile. The theory used was an incompressible, inviscid actuator disc analysis with the assumption that the hub/tip ratio is close to unity, reducing the problem to one of two dimensions. It was found that the velocity defects were attenuated across the rotor since the distorted flow is energized more than the undistorted flow by the rotor. Further, it was found that the theory proposed by Ehrich did predict the mean streamline shift with reasonable accuracy as well as the general shape of the downstream profile within the limits of the calculations and tests performed. Refinements in the theory, however, do appear to be in order, as the theory underestimated the distortion leaving the rotor by as much as 25%.

Thesis Supervisor: Alan H. Stenning

Title: Assistant Professor of Mechanical Engineering

Cambridge, Massachusetts
May 26, 1958

Professor Leicester F. Hamilton
Secretary of the Faculty
Massachusetts Institute of Technology
Cambridge 39, Massachusetts

Dear Professor Hamilton:

In accordance with the regulations of the faculty, I hereby submit a thesis entitled Circumferential Inlet Distortions in an Axial Flow Compressor in partial fulfillment of the requirements for the degree of Master of Science in Aeronautical Engineering.

Respectfully,

ACKNOWLEDGMENTS

The author wishes to express his appreciation to Professor Alan H. Stenning for his guidance and assistance as thesis advisor. The author is grateful for the suggestions and help offered by the Director of the Gas Turbine Laboratory, Professor Edward S. Taylor, and particular thanks are extended to Mr. Barry S. Seidel whose patient guidance as project leader was invaluable.

The graduate work for which this thesis is a partial requirement was performed while the author was assigned to the United States Naval Administrative Unit at the Massachusetts Institute of Technology.

This thesis was conducted under Gas Turbine Laboratory project number 7478 sponsored by the General Electric Company, the Westinghouse Electric Corporation, the Curtiss-Wright Corporation, and the Allison Division of the General Motors Corporation.

The many tests conducted were made with equipment expertly made by Mr. Paul Wassmouth and with probes made by Mr. Basil Kean. Much data taking and processing of data was capably performed by Mr. Joseph Jennings and Mr. A. Robert Brodsky. Typing of the final paper was performed by Natalie Appleton.

TABLE OF CONTENTS

Appendices

LIST OF TABLES AND ILLUSTRATIONS

SYMBOLS

Symbols

a	tangent α
b	tangent β
C_x	axial gas velocity
D	mean diameter of compressor
p	static pressure
p_o	total pressure
Q	volume flow rate, ft^3/sec
q	dynamic pressure
U	wheel speed
α	absolute flow angle
β	relative flow angle
$\bar{\varphi}$	$\bar{C}_x/U$, mean flow coefficient
ϕ	circumferential phase orientation of distortion
θ	angle measurement in circumferential direction
ψ	yaw angle

Subscripts

1	some distance upstream of the blade row
2	immediately in front of the blade row
3	immediately downstream of the blade row
4	some distance downstream of the blade

1. Introduction

Inlet velocity profile distortions in axial compressors have been a most important problem in high-speed gas turbine driven aircraft as these distortions reduce the performance of the over-all power plant by reducing the performance of the compressor. Such distortions may occur in flight under various conditions such as at off-design conditions, when the aircraft is flown at high angles of attack, or when the flow is turned or diffused too rapidly within the diffuser causing wall separation within the diffuser ducting. A distorted flow may also result because of a non-uniform compression at the inlet throat at supersonic speeds when the engine is operated at off-design conditions or when the aircraft is flown at high angles of attack. Further, circumferential inflow distortions have proved to be one of the most significant causes for the reduction in the stall margin of an axial compressor, and thus the study of such inlet conditions, their prevention, reduction, and attenuation has been the subject of several recent analytical publications, though little work has been done experimentally.

In the design of a compressor an understanding of the effects of a distortion and its attentuation makes it possible to design a compressor which is better able to withstand these effects. An investigation of the velocity diagrams of representative inlet stages shows that, in general, velocity profile defects will be reduced across the rotor because the distorted flow, or low energy region, is energized more than the undistorted flow by the rotor. The purpose of this present experimental investigation is to study the case of a single isolated rotor in an axial

flow compressor at different flow rates and with different inlet velocity profiles. The actual effect of the rotor on the inlet velocity profile was measured and the result compared with the downstream profile predicted by theories set forth in papers by Fredric Ehrich of the General Electric Company and George C. Ashby, Jr., of the NACA.

Erich's approach, which appears to be particularly satisfactory, is an actuator disc analysis. The self transport of vorticity is neglected in order to linearize the equations, and the analysis is restricted to the study of incompressible, inviscid flow with the assumption of a hub/tip ratio close to unity reducing the problem to two-dimensions. He had derived expressions giving the attenuation of the velocity distortion through the rotor and the circumferential shift in the profile as a function of the rotor geometry.

2. Equipment

2.1 Compressor

The compressor used in these tests and the test set up are shown in Figure 1. A single isolated rotor was used in all tests, and the characteristics of the compressor are presented in Reference 1. The compressor geometry is:

Outside radius	11.625 inches
Hub/tip ratio	0.75
Blade chord	1.00 inch
Blade aspect ratio	2.84

The blade-tip clearance was approximately 0.035 inches, and the blade sections were NACA 65-(12)10 airfoils with a stagger at the mean radius of 52.7 degrees measured from the axial direction. The cascade solidity was 1.02 at the leading edge, and there was linear twist of 9.70 degrees from the root to the tip. A schematic diagram of the compressor with the available pressure reading stations is shown as Figure 2.

2.2 Profile Generators

To generate the various inlet velocity profiles, screens of various solidities were used. Tests were first conducted with 22 1/2, 45, and 90 degree screens of high solidity, shown at the left of Figure 3, whereas the majority of the tests were conducted with one or two layers of window screening in a 45 degree screen holder, as shown on the right of Figure 3 with the screen holder, curved fences, and extension arm.

2.3 Instrumentation

The probes used for measuring yaw angle, static and total pressures were of the three hole Fecheimer tube type described in Reference 2. These probes have three 0.012 inch holes drilled through the rounded end of the tube at spacings of 42 degrees of arc with three hypodermic tubes contained inside a 0.125 inch stock tube. The middle hole points into the flow when the pressures at the outer two drillings are equalized. Probe calibration procedures and results are contained in Appendix A.

The yawing of the probes was accomplished through the use of a standard strain gage pressure transducer manufactured by the Statham Laboratories, Inc., of Los Angeles, California. Statham pressure transducers offer a simple means for the conversion of dynamic or static pressure into sensible electrical units. They are accurate and linear within $\pm$ 1% of full scale. The yaw angles were read with protractors mounted as shown in Figure 4 on the compressor shell. These protractors were aligned with a square using a known axial, flat surface on the outer wall of the compressor as a reference. The probes were aligned using the following optical technique. A small mirror was mounted on the shaft of each probe as seen in Figure 4 with the plane of the mirror being perpendicular to the axis of the center hole. A reference mirror was then aligned with the center line of the compressor using the axial, flat surface mentioned above. The mirror had a scribed vertical line and a "peep" hole which were used to bring into coincidence all images of the scribed line when looking through the "peep" hole at the mirror mounted on the probe. With this accomplished it was assured that the probe was aligned 90 degrees to the centerline of

the compressor and could then be locked into position with respect to the protractor. Similar procedures are employed in aligning interferometer mirrors.

Pressure measurements upstream and downstream were made through the use of a manifold pressure box, shown in Figure 1, and a strain gage pressure transducer connected to a D-C calibrating device which incorporates a transistorized D-C amplifier. This transducer equipment was manufactured by the Dynamic Instrument Company of Cambridge, Massachusetts. Some of the tests were run using a standard strain gage pressure transducer manufactured by the Statham Laboratories. A 32-tube inclined manometer board having a slope of 7.6 degrees and using red oil (specific gravity, 0.827) was used as stand-by equipment and for checking the pressure equipment described when necessary. This board was calibrated with a Prandtl micromanometer.

The damper position and the r.p.m. of the rotor controlled the volume flow of air through the compressor, and they were measured through the use of a counter mounted on the compressor control panel and an electrical strobotac respectively.

3. Investigation of an Inlet Total Pressure Distortion of Small Circumferential Extent

3.1 Experimental Procedure

For the experimental tests, the total pressure distortion generated by a one-inch diameter rod was measured upstream and downstream of the rotor. By using the measured upstream profile and a derived analytical equation for incompressible flow derived by George C. Ashby, Jr., in Reference 4, the profile downstream of the rotor was calculated and compared with the measured downstream conditions. The one-inch diameter rod was installed four inches upstream of the blade row of the rotor, the upstream probe one inch upstream of the rotor, and the downstream probe one inch downstream of the rotor. The cylinder was moved circumferentially through the use of an electrical traversing rig while the probes remained fixed in position. Readings were taken at two degree intervals of traverse.

3.2 Results and Discussion

Equation (2) of Reference 4 derived for incompressible flow is

$$dp_{o2} = dp_{o1} \left[\cos(\alpha_1 + \beta_1) \cos(\alpha_2 + \beta_2) \frac{\cos \alpha_1 \cos \beta_2}{\cos \beta_1 \cos \alpha_2} \right]$$

Ashby states that when the total pressure deficit between the undisturbed flow and a point in the disturbed flow upstream of the rotor and the velocity diagram for the undisturbed flow are known, the downstream total pressure deficit can be determined using the above equation. The distortion must be of small circumferential extent however, so that the undistorted flow dictates the static pressure field in the blade passage.

Figure 5 shows the measured upstream total pressure profile and the measured and predicted profiles downstream of the rotor. This theory failed to predict the downstream profile with any reasonable accuracy. Figure 4 of Reference 4 showed similar results with the measured downstream profile showing a larger attenuation and wider circumferential disturbance than was predicted by the theory.

Ashby asserts that reasonable accuracy is obtained when the static pressure field in the blade passage is altered by a distortion of large circumferential extent. That this is not the case has been determined by several tests, one of which is exemplified by Figure 6 which shows the measured total pressure distortions upstream and downstream of the rotor and the calculated downstream profile using a 45 degree window screen.

3.3 Conclusions

A single experimental investigation of the effect of an isolated rotor on a known inlet total pressure distortion in an axial flow compressor and a comparison of this effect with that predicted by a theoretical equation derived in Reference 4 has been conducted. The predicted downstream conditions compared unfavorably with the measured conditions, and therefore it was concluded that Ashby's theory as set forth in Reference 4 is not practical for predicting significant inlet distortions.

4. Velocity Profile Generation

In the first experiments conducted, the screens of various solidities were tested. These screens were traversed manually with the probes left stationary. Upon taking data however with the 45 degree screen of highest solidity, it was found that the direction of the flow upstream of the rotor was changed radically from essentially axial to a maximum of sixty degrees from axial. The resulting inlet velocity profile is shown on Figure 7. It was noted that the defect was not symmetrical, having a larger velocity on the side down from the direction of rotation. The cause and remedy of this asymmetry was later investigated. It was also noted in this profile that there were two larger reductions in the axial velocity at the edges of the distortion giving the profile an appearance of a "W". As the screen holder width is one-eighth of an inch and is located three to five inches upstream from the measuring probe, it was concluded that the W-shape was not caused by the sides of the screen holder as any wake caused by the holder would be dissipated prior to progressing downstream to the probe, 24 or more chord lengths away. As the tests with and without fences both give the characteristic W-shape, it was further concluded that the curved fences which may cause thickening of the boundary layer did not cause this irregular shape. As the width of the distortion was roughly the width of the screen, it was deduced that the edges of the screen (or the screen holder) were generating vortex sheets which were extending downstream causing the increased defect due to the direction of the circulation in the vortex sheet. This

is in agreement with theory as stated in Reference 7 which shows a plot of velocity versus distance for a pair of point vortices as

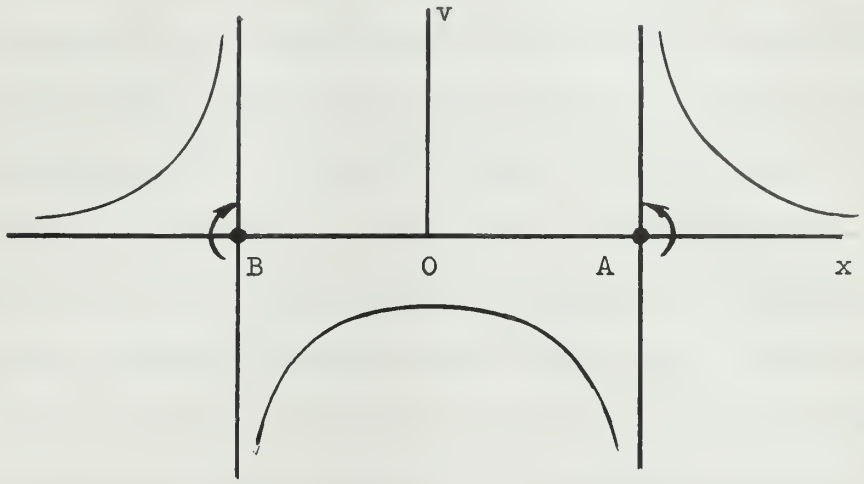

Tests were discontinued with these screens, as the profiles generated would be unsuitable for comparison with a small perturbation theory used in Reference 5 due to the large divergence of the flow.

To reduce the blockage and consequently the absolute angle of flow, window screening was used. Again, however, the angles were too large to be considered within the limits of small perturbation theory. These limits were set as five degrees either side of axial.

Fences were attached to the screen holder in a manner shown in Figure 3 to reduce the divergence angle. This brought the angles within ten degrees of axial, and finally less than five degrees when the fences were curved upstream to align them roughly with the streamlines to prevent the divergence of the flow at the leading edges of the fences. The fence was first attached with twelve inches extending upstream and nothing downstream giving the profile shown on Figure 8. The straight fence

with twelve inches extending upstream and six inches downstream gave the resulting profile plotted on Figure 9.

A further modification which improved the results was the shortening of the upstream fence to five inches and extending the downstream one inch. With this design, several tests were made for one and two layers of window screening, various flow coefficients, and volume rates. These results are shown on Figures 10, 11, 12, and 13. These figures all showed the asymmetry of the first profiles and the characteristic W-shape due to the vortex sheets emanating from the edges of the screen. The probe locations, the volume flow rates, the flow coefficients, and certain remarks for all the runs are contained in Table I for convenient reference with Figure 15 explaining column headings.

Due to the proximity of the rotor to the screen and probe, it can be concluded that the asymmetry of the various profiles was due to rotor effect. Since actuator disc theory shows that rotor influence diminishes exponentially with distance from the rotor, an attempt was made to reduce the asymmetry by extending the screen upstream eight inches and moving the probe upstream ten inches. The screen was extended by attaching an arm shown in Figure 3 of length eight inches. The asymmetry was slightly reduced, but not by a significant amount. A further attempt to solve this problem was the installation of two screens 180 degrees apart from one another at this extended position. The theoretical effect of this attempt is contained in Appendix B. The profile generated by this arrangement is shown on Figure 14, and shows again that the rotor effect is still present. It was then concluded that a symmetrical profile must be generated by modifying the screening to compensate for the effect of the rotor rather than trying to eliminate it.

5. Investigation of Velocity Profile Distortions of Significant Circumferential Extent

5.1 Analytical Procedure

From the several inlet distortions of Figures 7 through 13, two were selected to be analyzed using the theory proposed by Ehrich in Reference 5. These two were those shown in Figures 11 and 13 with flow coefficients of 0.440 and 0.538 respectively. In the test of Figure 11 two layers of window screening were used and in that of Figure 13, one layer.

With the W-shape inlet profiles obtained by tests, it was found that more Fourier coefficients were needed to duplicate the inlet profile than was deemed practicable to handle in the analysis. Therefore, as this W-shape was caused by vortex sheets which probably wash out or which are undoubtedly washed out by the rotor, an assumed smooth curve was faired in thus eliminating these irregularities caused by the vortex sheets. The assumed alterations of the inlet profiles are shown as dashed lines on Figures 16 and 17.

The Fourier coefficients were obtained by using the Dent-Draper rolling sphere harmonic analyzer manufactured by the Mico Instrument Co. of Cambridge, Massachusetts. It was found that the inlet profile could be duplicated closely at most points with ten harmonics, but that several of the points required twenty harmonics to reproduce the curve with reasonable accuracy. These calculated points are shown on Figures 16 and 17 as crosses, and it can be seen that they reproduce the profile with about ten per cent accuracy. It was assumed that this accuracy was maintained in the analysis for finding the downstream profiles. This seemed

reasonable as the inlet coefficients were only operated on by analytical expressions set forth in Reference 5.

Figures 16 and 17 show the measured upstream and downstream profiles, the calculated downstream profile, the experimental points for the upstream and downstream profiles, and the calculated upstream and downstream points used in this analysis.

5.2 Discussion

In Ehrich's theory, an expression for $\tan \phi_4$ is given. This expression, however, does not allow one to determine the principal values of ϕ_4. Small changes in the denominator of the expression for $\tan \phi_4$ when ϕ_4 is near ± 90 degrees can cause the sign of the tangent to change. As small changes should not cause large phase angle differences such as from +90 degrees to -89 degrees, it was concluded that the angle must either lie within the first and second quadrants or within the third and fourth quadrants, either region allowing $\tan \phi_4$ to take on all values from $-\infty$ to $+\infty$. As Reference 5 gives an example of -40 degrees for the phase angle, it was concluded that Ehrich meant for the angle ϕ_4 to range only from 0 to -180 degrees. This is also in agreement with one's intuition in regards to phase shift in a three-dimensional case with a rotor of finite thickness.

From Figures 16 and 17, it is apparent that the theory does predict the phase shift with a considerable degree of accuracy. The general shape of the profile also appears to be correct but the magnitudes were not predicted with similar accuracy. Part of this difference may lie in the fact that too few harmonics were used in the calculations.

5.3 Conclusions and Suggestions for Future Work

It is believed that Ehrich's theory predicts with reasonable accuracy the phase shift of the mean streamlines through an isolated rotor. It further appears that his theory predicts the general shape of the downstream profile, but may need certain refinements to bring the magnitude of the defect into closer agreement with the measured defect. This may be rectified in future work using higher flow coefficients and varying solidity screens, as it was noted that in Figure 17 with a flow coefficient of 0.538, closer correlation resulted than in Figure 16 with a flow coefficient of 0.440. In the example used by Ehrich, the flow coefficient was equal to 1.00 indicating that the tests conducted may be near the limits of $\bar{\varphi}$ for the theoretical predictions to be valid.

It is therefore suggested that future tests be conducted with the results of this thesis as a basis for the selection of flow coefficients, volume flow rates, rotor speeds, screening to be used, and locations for taking measurements. It is further suggested that the Fourier coefficients be calculated on the IBM 704 computer (for example, E2PK 4EA1, Fourier series coefficient sub-routine) to increase the accuracy of the computations and to reduce the laborious calculations required in operating on ten to twenty harmonics. To help reduce the number of terms required in the series, it is suggested that the inlet distortion be altered by making a screen of varying solidity which would eliminate the W-shape and perhaps make the profile symmetrical.

TABLE I

Fig.	Obstruction	a	b	c	d	$\bar{\varphi}$	Q $\frac{ft^3}{sec}$	Remarks
10	45°window screen (two layers)	3"	14"	9"	39° arc	0.319	36.7	5"curved fence upstream and 1" curved fence downstream
8	45°window screen (one layer)	5"	4"	9"	0°	0.364	36.6	12"curved fence upstream and no fence downstream
9	45°window screen (one layer)	5"	4"	9"	0°	0.391	39.4	12"straight fence upstream and 6" fence downstream
15	Two 45°window screens separated by 180°(one layer each)	3"	14"	9"	39°	0.413	48.8	No fences
11	45°window screen (two layers)	3"	14"	9"	39°	0.440	50.6	Same as Fig. 5
12	45°window screen (two layers)	3"	14"	9"	39°	0.481	48.4	Same as Fig. 5
7.	45°screen (highest solidity)	5"	4"	9"	0°	0.501	60.5	No fences
13	45°window screen (one layer)	3"	14"	9"	39°	0.538	54.3	Same as Fig. 5

APPENDIX A

PROBE CALIBRATION

Probe calibration was carried out in the Gas Turbine Laboratory probe calibration tunnel which was used in the experimental work of Reference 6. Figure 18 shows the total pressure gradient measured. This measured profile was in close agreement with the profile obtained from Reference 6, as can be seen on Figure 18.

The procedure used in measurement was to yaw the three-hole probe until the static pressure taps were equalized. The resulting yaw angle, ψ, the total pressure, and the static pressure were read, with the pressures being read on the Dynisco pressure reading apparatus.

The constant for probe "A" in the expression for yaw angle correction,

$$\Delta\psi = C \frac{\partial p_0/\partial y}{p_0 - p}$$

obtained from Reference 6, was determined to be 3.67, and 3.72 for probe "B". The angles obtained using the three-hole probes checked extremely closely with angles obtained in the experiments of Reference 6. As the total pressure gradient was measured in the compressor and was found to be small, (relative to the size of the probe) a correction for the yaw angle measurements was unnecessary. Also, since the total pressure gradient in the compressor was small and the yaw angles accurate, corrections

for total pressure were considered negligible. The static pressures, however, were corrected, as the static holes in the Fecheimer tube were not drilled at the location at which free stream static pressure theoretically exists. Machining problems prevented the choice of this location. Figure 19 shows a plot of $(p_{indicated}-p_{wall}/q)$ versus vertical traverse in the calibration tunnel. This plot gave the results that for probe "A"

$$\frac{p_{true} - p_{probe}}{q} = 0.132$$

For probe "B":

$$\frac{p_{true} - p_{probe}}{q} = 0.083$$

APPENDIX B

CHOICE OF DISTORTION WAVE LENGTH AND ITS DISTANCE FROM THE ROTOR

In the analytical investigation of Reference 5, it was shown that any circumferential distortion of width, $2\pi r/n$, will induce local disturbances at the rotor. These disturbances will die away to a value of exp - 2π upstream and downstream of the rotor in an axial distance equal to the width of the distortion .

For the tests conducted the distortion width is

$$\text{distortion width} = 2\pi r/n = 20\pi$$

$$\text{therefore } \frac{r}{n} = 10$$

The decay term in the attenuating process is

$$e^{-\frac{nx}{r}}$$

and thus with the probe located four inches upstream of the rotor, the rotor influence, or disturbance, is reduced by

$$\exp(-0.4) = 0.67$$

Increasing x to nine inches by moving the probe upstream causes the disturbance to diminish to

$$\exp(-0.9) = 0.406$$

An alternative method for decreasing the rotor influence is to change the period or distortion width by introducing a second screen located 180 degrees away from the first. Thus: $\frac{2\pi r}{n} = 10\pi \quad \frac{r}{n} = 5$ and with x = 9" the disturbance diminishes theoretically to

$$\exp(-1.8) = 0.1651$$

APPENDIX C

A SUMMARY OF EHRICH'S THEORY FOR AN ISOLATED ROTOR

From Reference 5, for an inlet profile defined by

$$C_{x_1} = \bar{C}_x + \sum_n (\epsilon_1)_n \sin\left[\frac{n\theta}{2\pi} + (\varphi_1)_n\right]$$

the velocity at the exit for an isolated rotor (referred to the same mean streamline) will be given by

$$C_{x_4} = \bar{C}_x + \left(\frac{\epsilon_4}{\epsilon_1}\right)\sum_n (\epsilon_1)_n \sin\left[\frac{n\theta}{2\pi} + (\varphi_1)_n + \varphi_4\right]$$

where the rotor attenuation is given by

$$\left(\frac{\epsilon_4}{\epsilon_1}\right) = \left\{\frac{(1+a_1^2)(1+b_2^2)(1+b_3^2)}{(1+a_4^2)\left[4(b_3-a_4)^2+(1+b_3^2)^2\right]}\right\}^{\frac{1}{2}}$$

and the phase angle shift is given by

$$\tan\varphi_4 = \frac{(b_3-a_4)\left\{(1+b_3^2)\left[(1+a_4b_3)+(1+a_1b_2)\right]+2(b_3-a_4)^2-2(1+a_4b_3)(1+a_1b_2)\right\}}{(b_3-a_4)^2\left\{-2\left[(1+a_4b_3)+(1+a_1b_2)\right]+(1+b_3^2)\right\}-(1+b_3^2)(1+a_4b_3)(1+a_1b_2)}$$

where

$a_1 = \tan\alpha_1$ $\qquad$ $a_4 = \tan\alpha_4$

$b_2 = U/\bar{C}_x$ $\qquad$ $b_3 = b_2 + a_4 - a_1$

$(b_3 - a_4) = U/\vec{C}_x$

For the data of Figure 16:

$$\left(\frac{\epsilon_4}{\epsilon_1}\right) = 0.7348$$

$$\varphi_4 = -75°6$$

For the data of Figure 17:

$$\left(\frac{\epsilon_4}{\epsilon_1}\right) = 0.7077$$

$$\varphi_4 = -88°0$$

APPENDIX D

BIBLIOGRAPHY

Ref. 1: Moore, R. W. and Schneider, K. H., "Measurement of Flow through a Single-stage Axial Compressor", M.I.T. Gas Turbine Laboratory Report 27-6, December 1954.

Ref. 2: Horlock, J. H., "Instrumentation Used in Measurement of the Three Dimensional Flow in an Axial Flow Compressor", Aeronautical Research Council Current Paper No. 321, London, March 1955.

Ref. 3: Rannie, W. D. and Marble, F. E., "Unsteady Flows in Axial Turbomachines", Guggenheim Jet Propulsion Center, C.I.T. Publication No. 94.

Ref. 4: Ashby, G. C., Jr., "Investigation of the Effect of Velocity Diagram on Inlet Total-pressure Distortions Through Single-stage Subsonic Axial-flow Compressors", NACA Research Memorandum L57A03, 17 April 1957.

Ref. 5: Ehrich, F., "Circumferential Inlet Distortions in Axial Flow Turbomachinery", Journal of Aeronautical Sciences, June 1957.

Ref. 6: Lima, H., "Yaw Probes in a Total Pressure Gradient", M.I.T. S.M. Thesis in Mechanical Engineering, January 1958.

Ref. 7: Milne-Thomson, L. M., Theoretical Aerodynamics, 2nd Edition, D. Van Nostrand Co., Inc., New York, 1952.

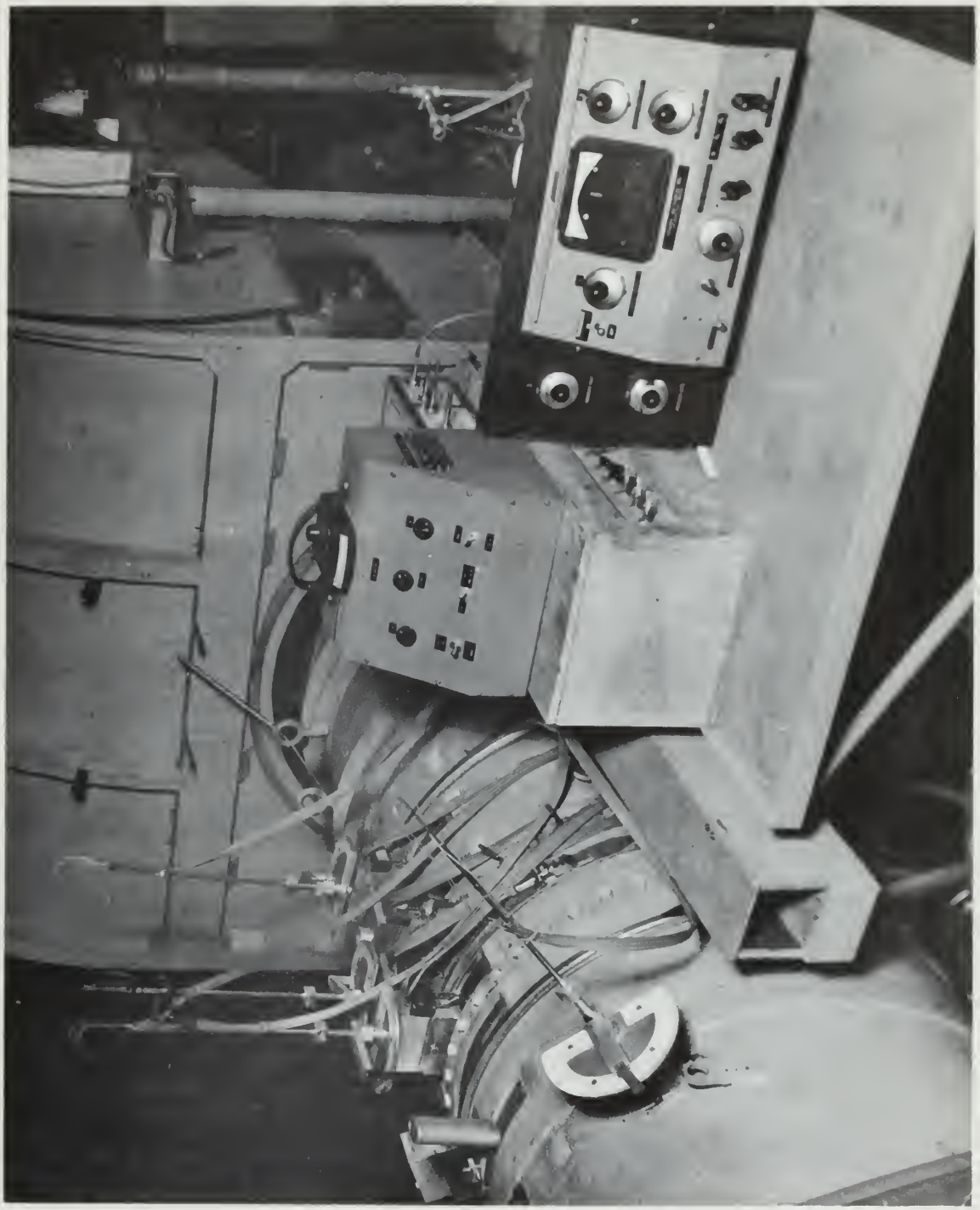

FIG. 1 — SET-UP OF TEST APPARATUS

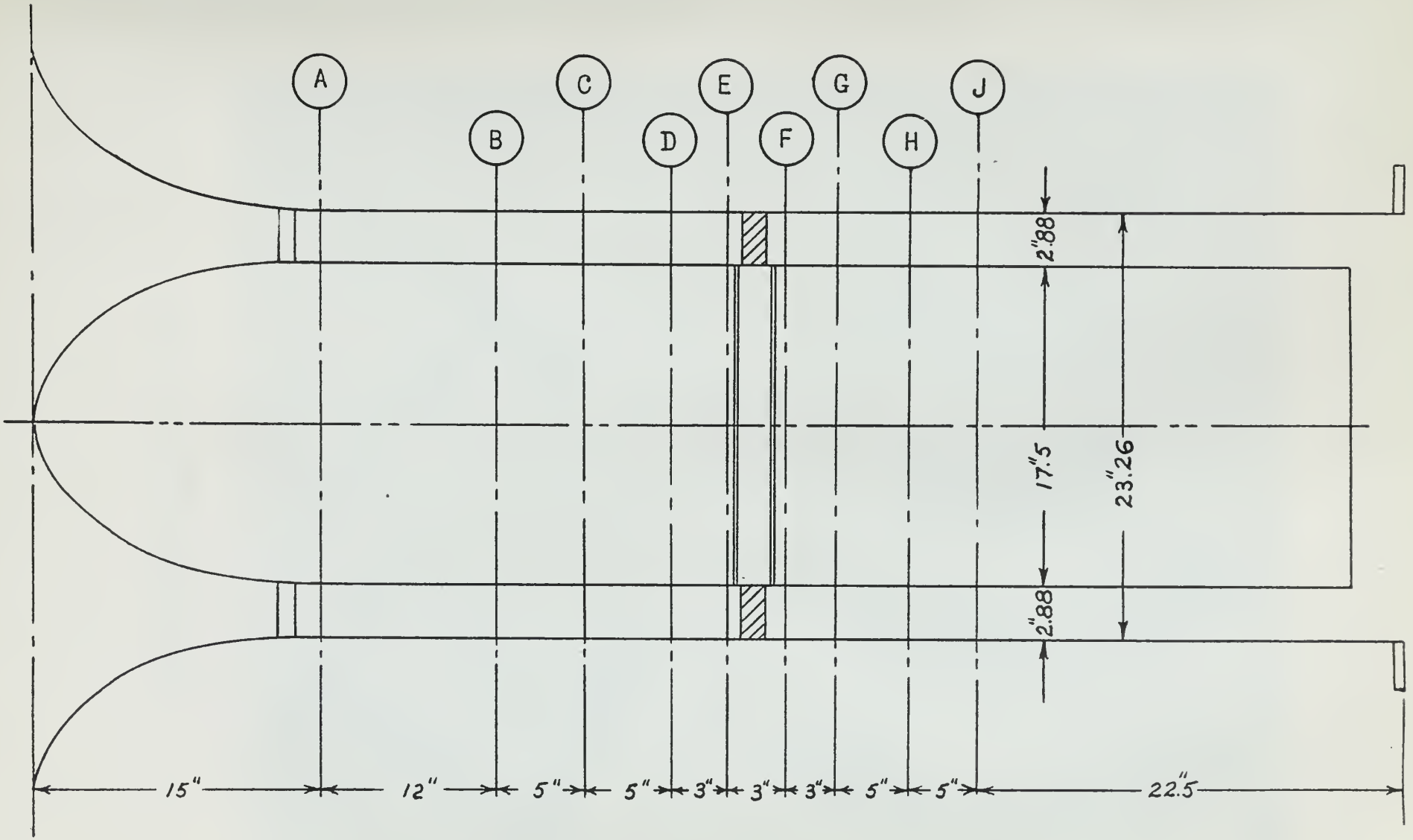

FIG. 2 — DIAGRAM OF THE COMPRESSOR

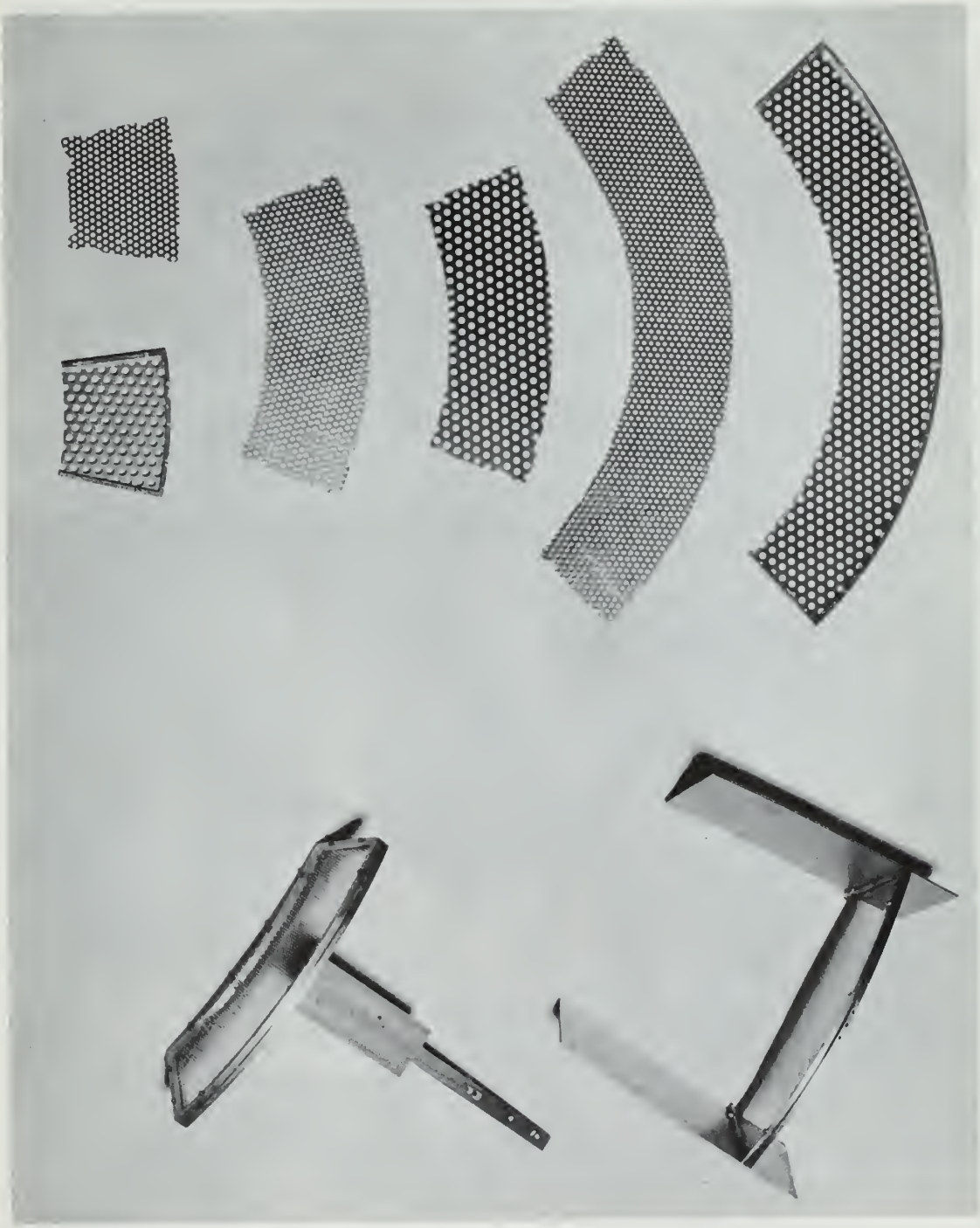

FIG. 3 — PROFILE GENERATORS

FIG. 4 — PROBE ARRANGEMENT

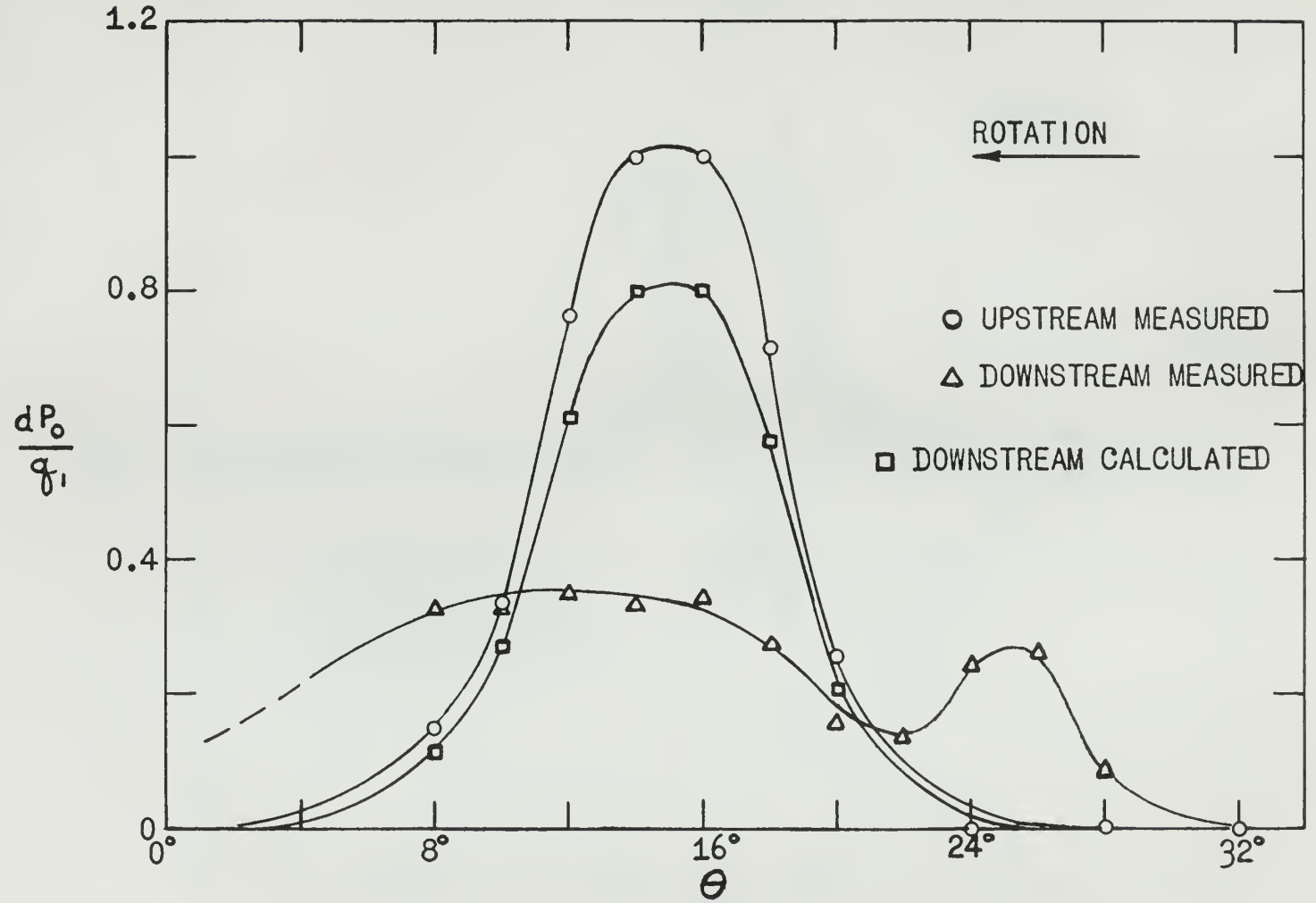

FIG. 5 — TOTAL PRESSURE PROFILE (CYLINDER)

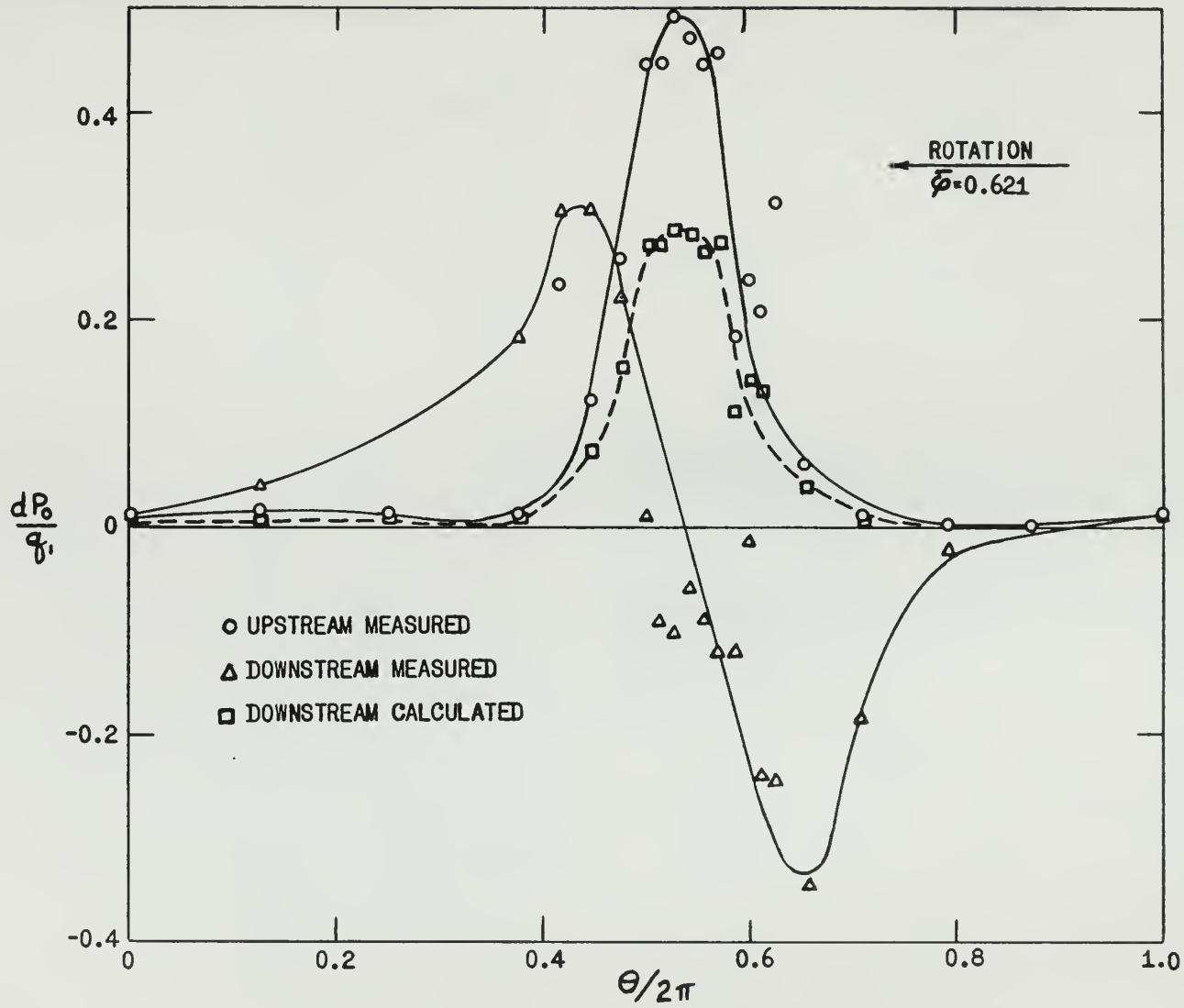

FIG. 6 — TOTAL PRESSURE PROFILE (SCREEN)

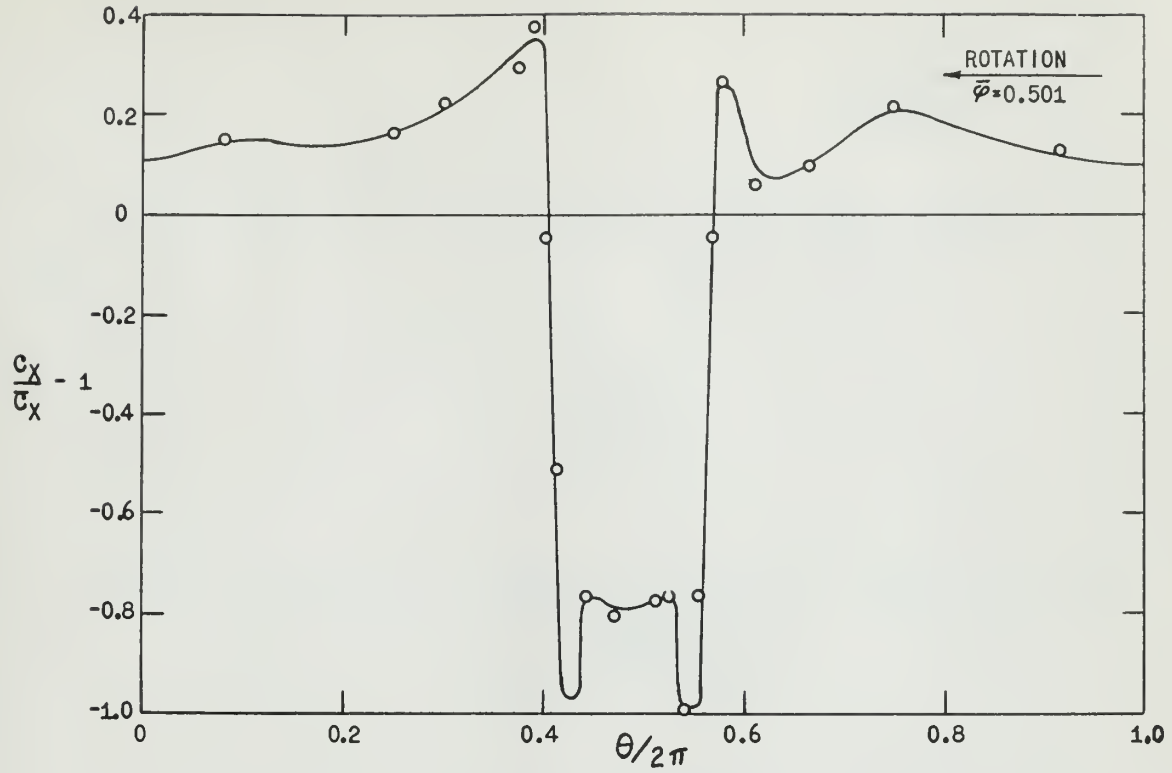

FIG. 7 — UPSTREAM PROFILE

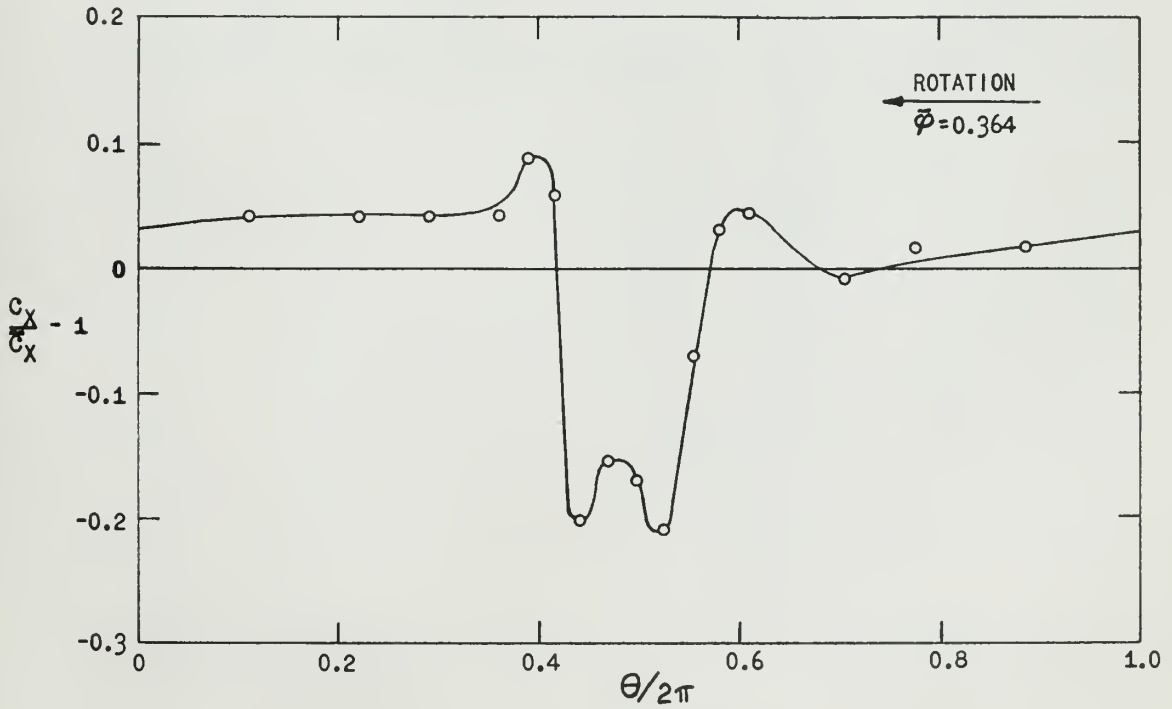

FIG. 8 — UPSTREAM PROFILE

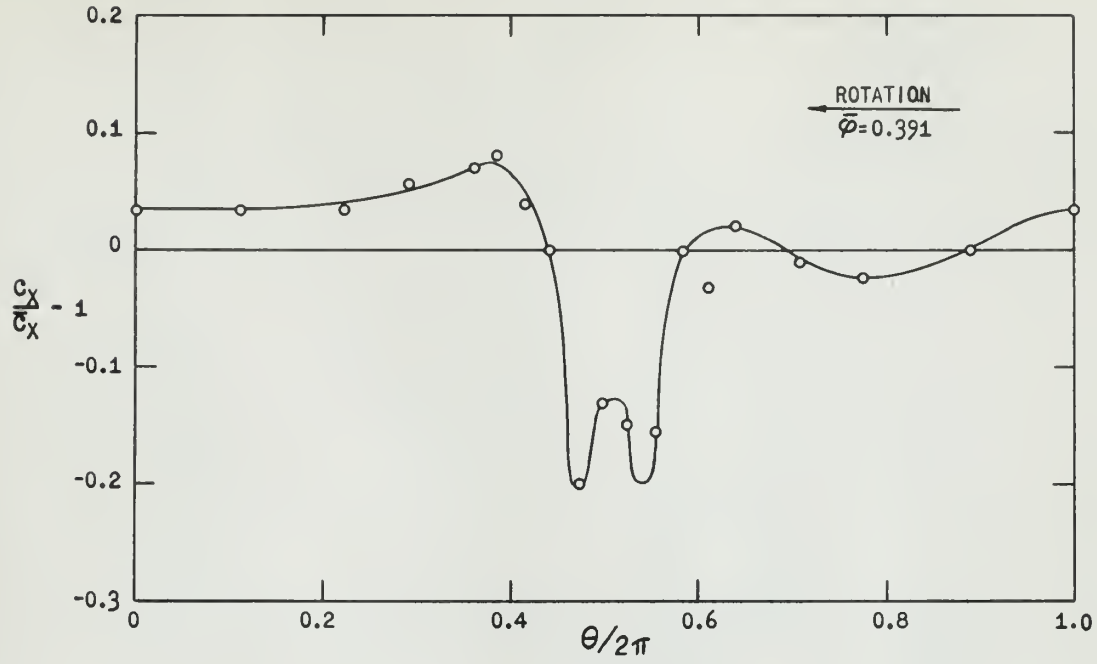

FIG. 9 — UPSTREAM PROFILE

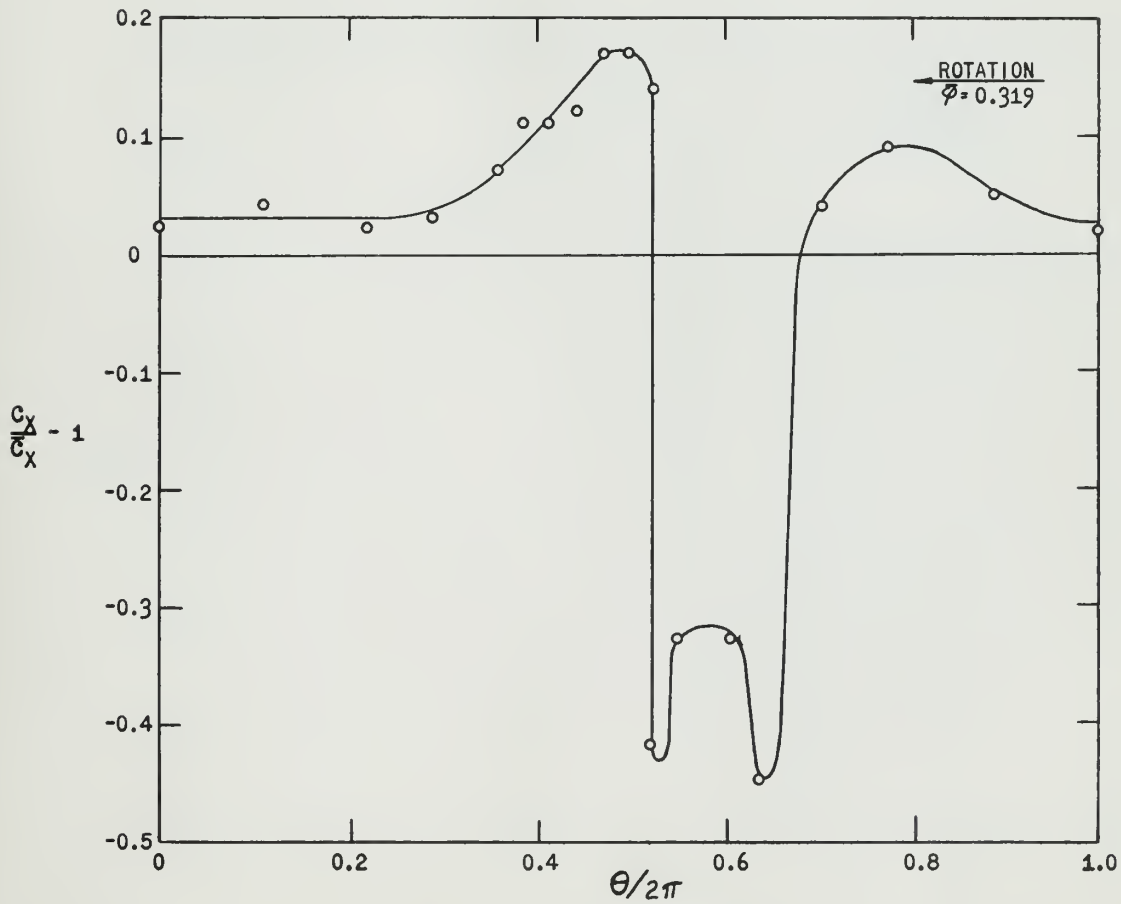

FIG. 10 — UPSTREAM PROFILE

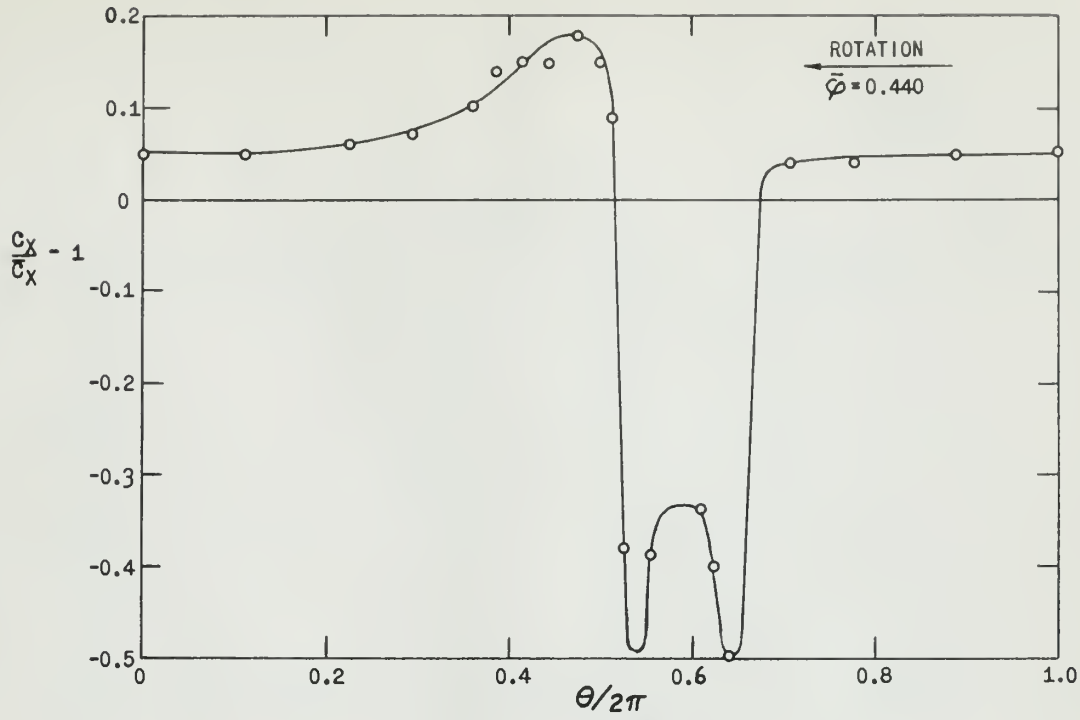

FIG. 11 — UPSTREAM PROFILE

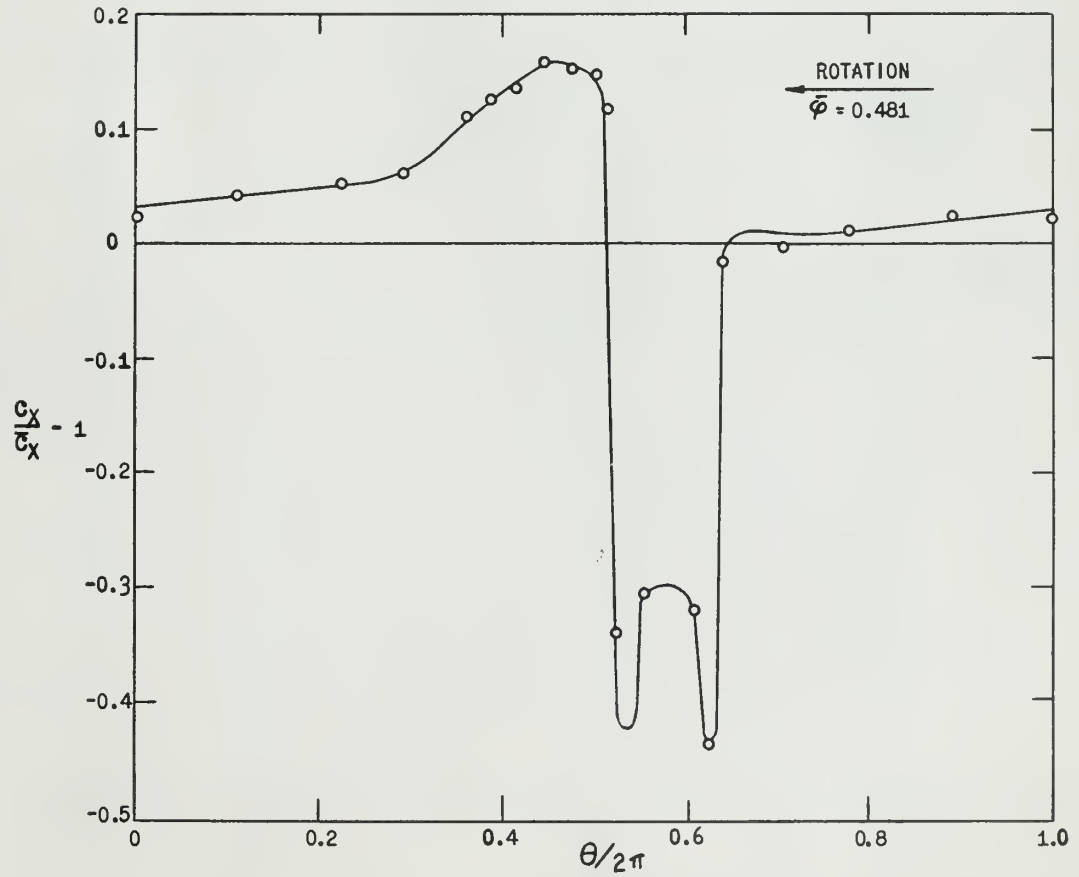

FIG. 12 -- UPSTREAM PROFILE

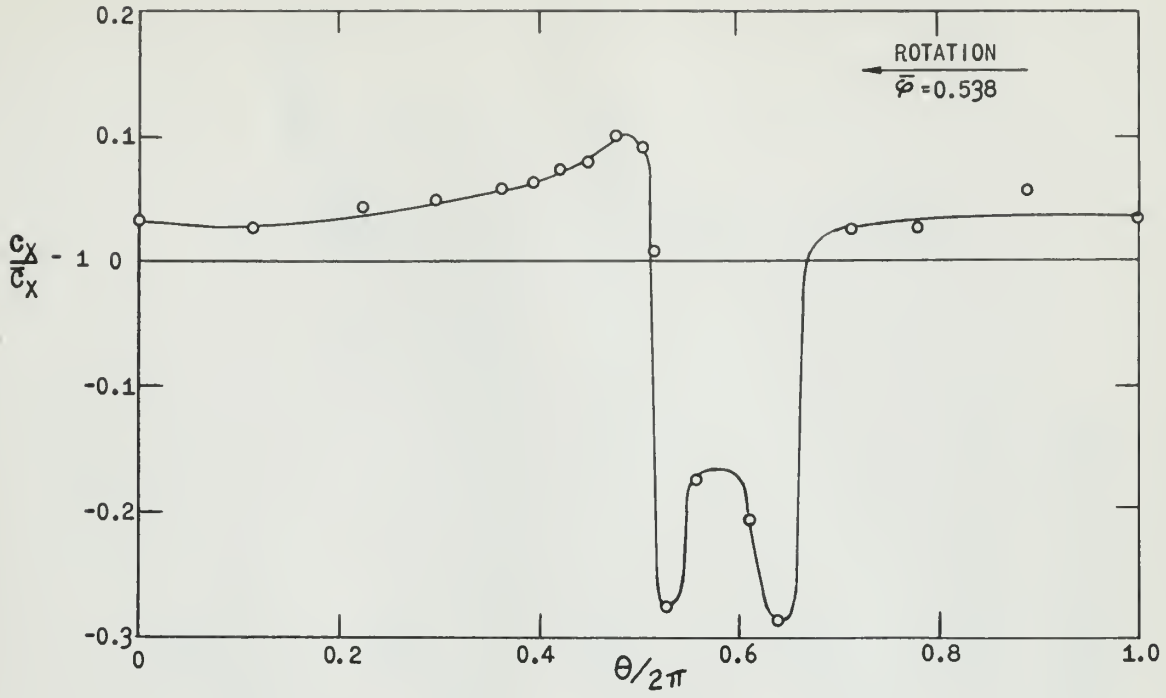

FIG. 13 — UPSTREAM PROFILE

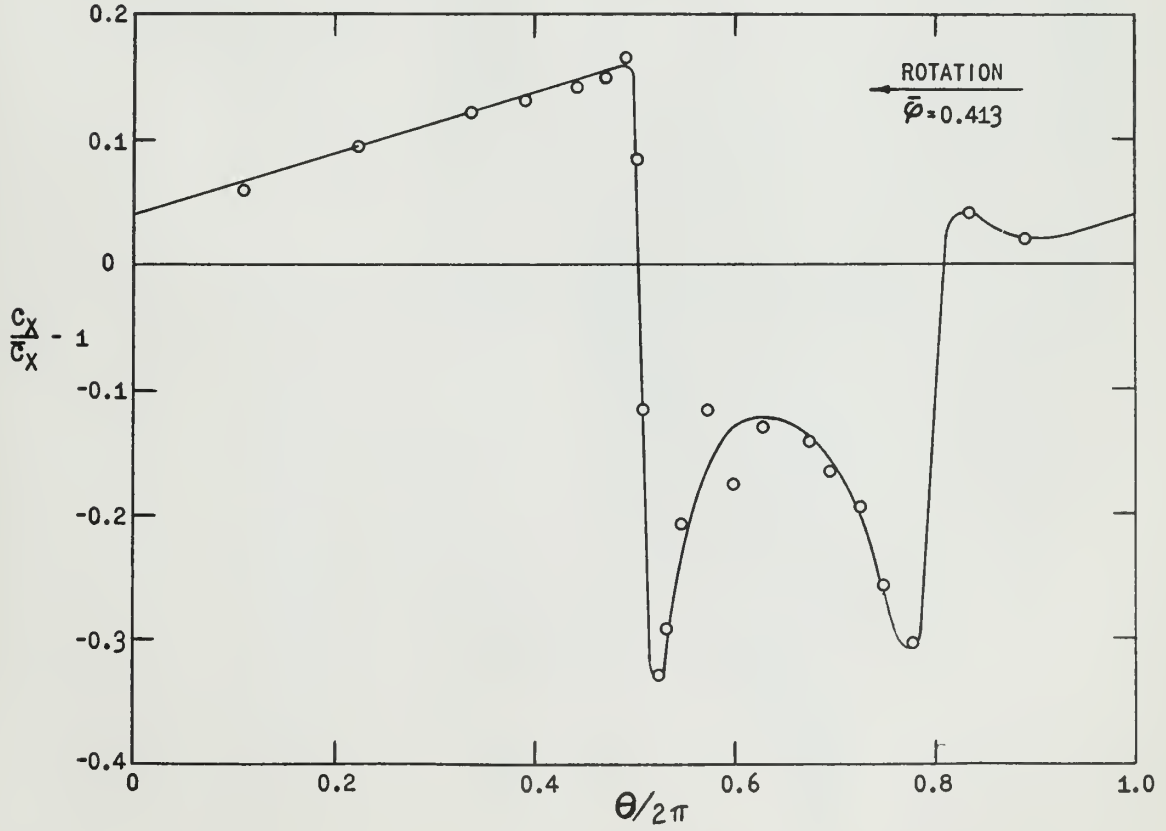

FIG. 14 — UPSTREAM PROFILE

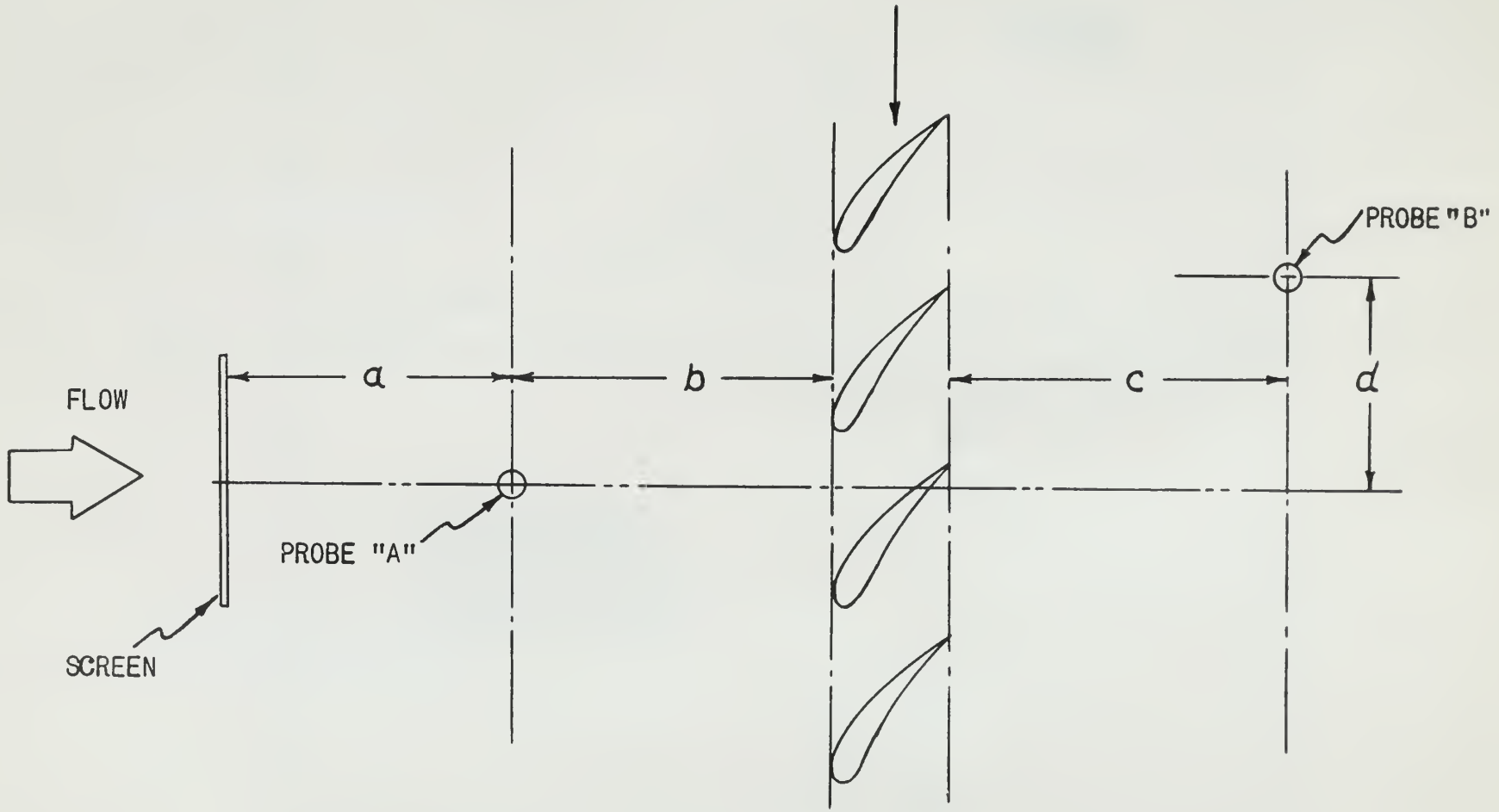

FIG. 15 — MEASUREMENT REFERENCE POSITIONS

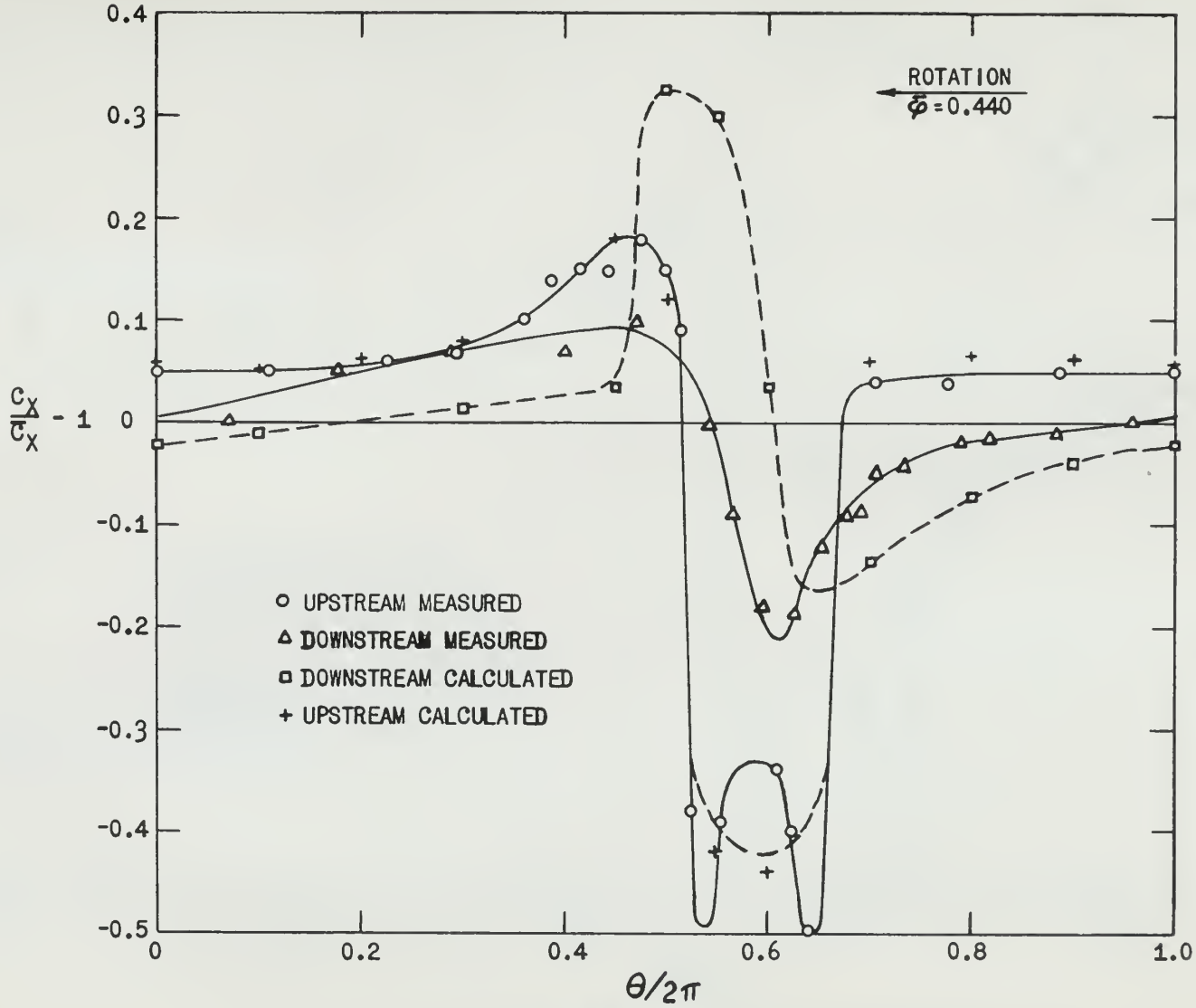

FIG. 16 — MEASURED AND PREDICTED PROFILES

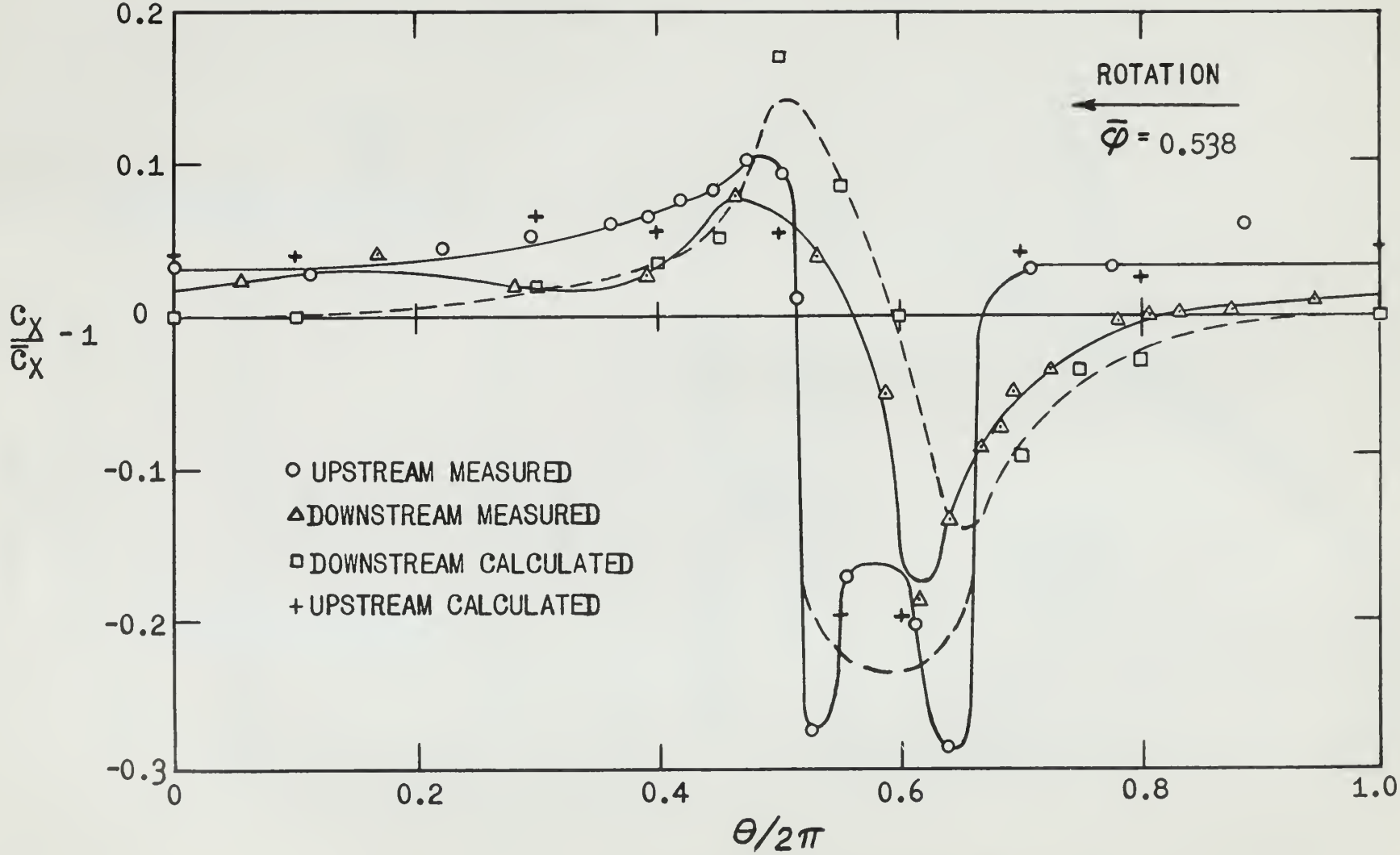

FIG. 17 — MEASURED AND PREDICTED PROFILES

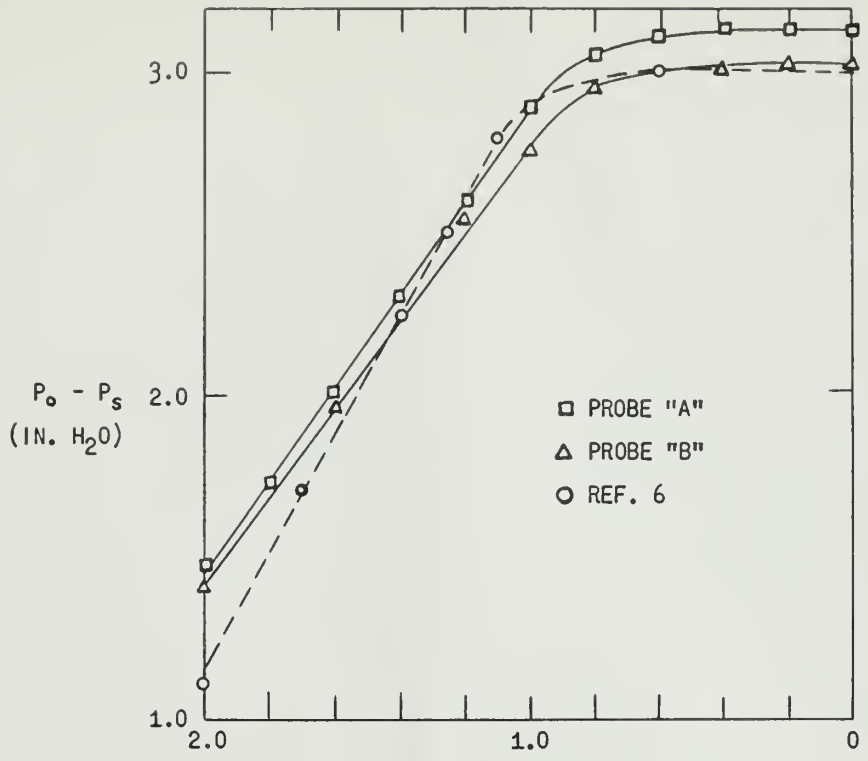

FIG. 18 — CALIBRATION TUNNEL TOTAL PRESSURE GRADIENT

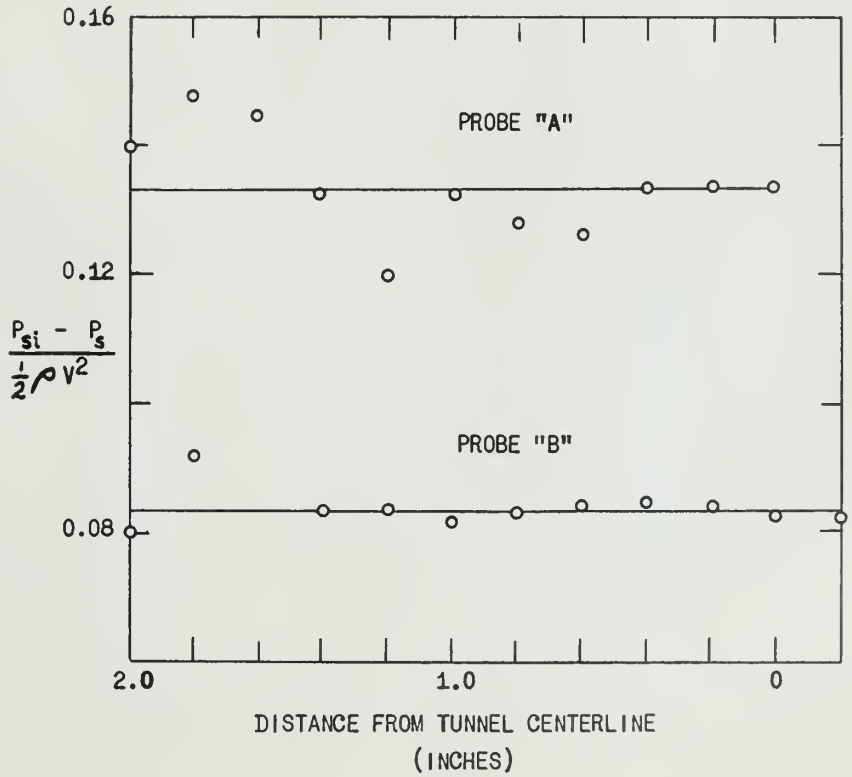

FIG. 19 — PROBE CALIBRATION